www.saltworkconsultants.com

Salty Matters

John Warren - Thursday May 31, 2018

Stable isotopes in evaporite systems: Part II - $\delta^{13}C$ (Carbon)

Introduction

^{13}C interpretation in most ancient basins focuses on carbonate sediment first deposited/precipitated in the marine realm. Accordingly we shall first look here at the significance of variations in ^{13}C over time in marine carbonates and then move our focus into the hypersaline portions of modern and ancient salty geosystems. In doing so we shall utilize broad assumptions of homogeneity as to the initial distribution of ^{13}C (and ^{18}O) in the marine realm, but these are perhaps oversimplifications and associated limitations need to be recognized (Swart, 2015)

In the next article we shall look at the utility of crossplots of carbon and oxygen isotopes. Stable oxygen isotope values ($\delta^{18}O$) crossplotted with respect to carbon isotope values ($\delta^{13}C$) from, the same sample creates one of the most widely applied proxies used to infer palaeo-environmental conditions (depositional and diagenetic) in Holocene and ancient carbonate sediments. This is in large part due to kinetic fractionations that occur during evaporation (Leng and Marshall, 2004). It has long been known that as any liquid evaporates, the residual fluid becomes enriched in the less abundant heavy isotope(s) (see Horton et al., 2016 for detailed discussion).

Interpreting 13C

Over the Phanerozoic the standard paradigm for interpreting variations in variations in ^{13}C values from modern and ancient marine carbonate is based on an integration of our understanding of the carbon cycle with the following arguments. Most of the carbon in Earth's near-surface systems is stored in sedimentary rocks with only about 0.1% in living organisms and the atmosphere-hydrosphere (Figure 1). Oxidized carbon occurs primarily as marine carbonates and reduced carbon as organic matter in sediments. In the carbon cycle, CO_2 from the oceans and atmosphere is transferred into sediments as carbonate carbon (C_{carb}) or organic carbon (C_{org}), the former of which monitors the composition of the oceans (Figure 1). The cycle is completed by uplift and weathering of sedimentary rocks and by volcanism, both of which return CO_2 to the atmosphere.

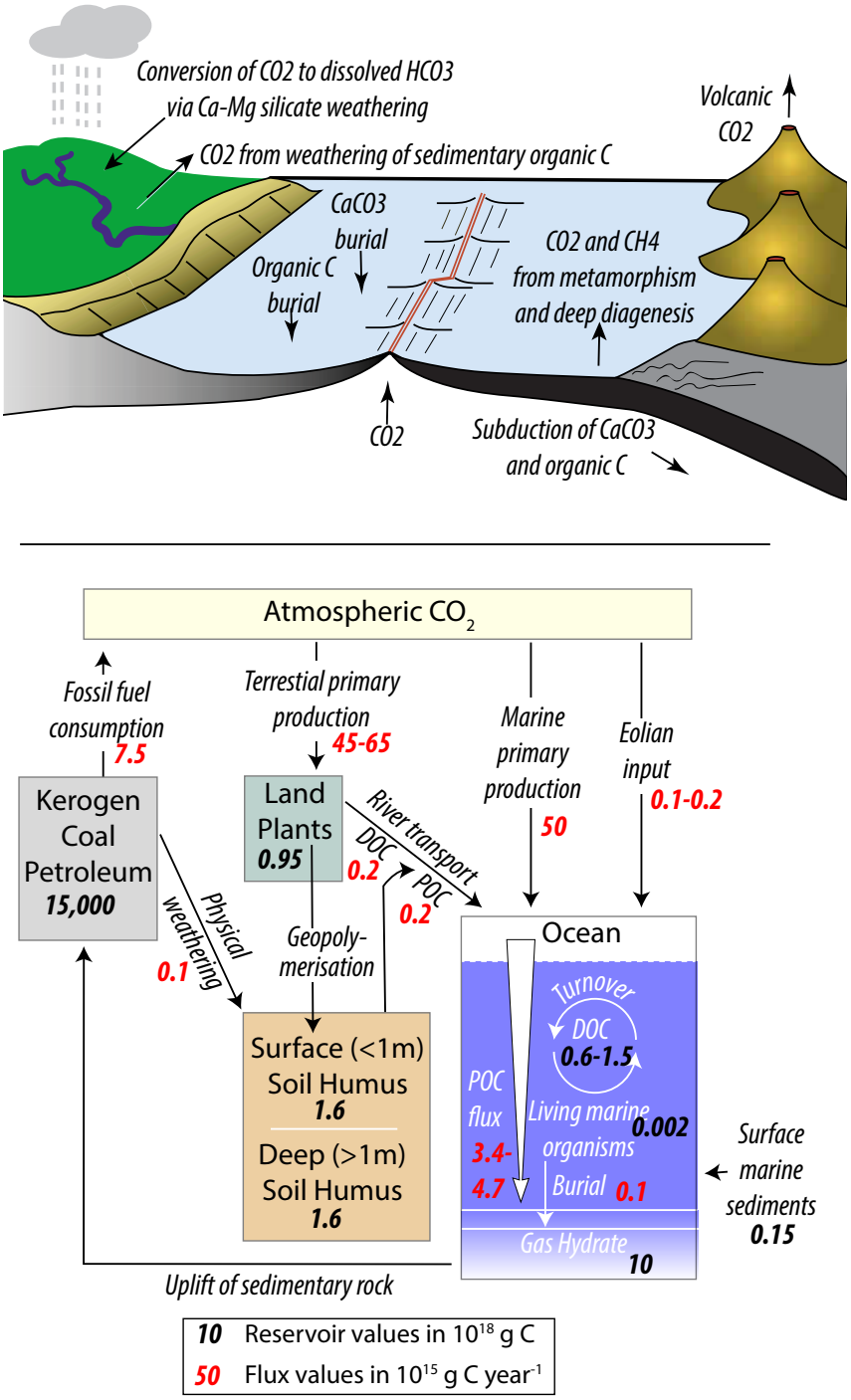

Figure 1. Flux volumes in the modern carbon cycle.

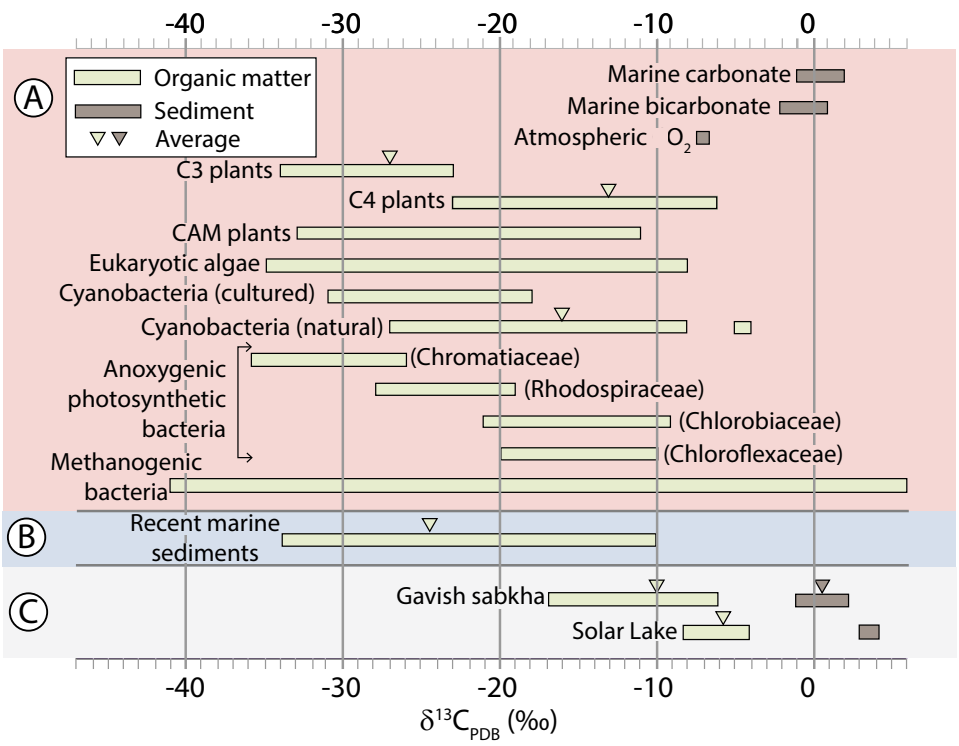

Figure 3. Carbon isotope ranges in a variety of organic and sedimentary materials (After Schidlowski et al., 1984). Not that sediments in the Solar Lake salina and Sabkha Gavish show elevated values.

There are two stable carbon isotopes, carbon 12 (6 protons and 6 neutrons) and carbon 13 (6 protons and 7 neutrons). Photosynthetic organisms incorporate disproportionately more CO_2 containing the lighter carbon 12 than the heavier carbon 13 (the lighter molecules move faster and therefore diffuse more easily into cells where photosynthesis takes place). During periods of high biological productivity, more light carbon 12 is locked up in living organisms and in resulting organic matter that is being buried and preserved in contemporary sediments. Consequently, due the metabolic (mostly photosynthetic) activities of a wide variety of plants, bacteria and archaea, the atmosphere and oceans and their sediments become depleted in carbon 12 and enriched in carbon 13 (Figure 2)

It is assumed that the carbon isotopic ratio in calcareous shells of marine organisms is in equilibrium with that of seawater. So as more carbon 12 is held in biomass during times of high primary productivity, and increased burial of organic carbon, calcareous ($CaCO_3$) skeletal materials become enriched in carbon 13. In contrast during periods of low biological productivity and decreased burial of organic carbon, for example following mass extinctions, marine calcareous skeletal materials become enriched in carbon 12.

Hence plotting variations in carbon isotopes in marine carbonates and organic matter over time offers a way to trace the growth of the crustal reservoir of reduced carbon (Des Marais, 1997). That is, the relative abundance of carbon isotopes is controlled chiefly by: 1) equilibrium isotopic effects among inorganic carbon species, 2) fractionation associated with the biochemistry of organic matter, and 3) the relative rates of burial of carbonate and organic carbon in sediments (Condie 2016).

Because organic matter preferentially incorporates ^{12}C over ^{13}C, there should be an increase in the $^{13}C/^{12}C$ ratio (as measured by $\delta^{13}C$) in buried carbon with time, and indeed this is what is observed (Des Marais, 1997; Worsley & Nance, 1989). $\delta^{13}C_{org}$ increases from values < -40‰ in the Archaean to modern values of -20 to -30‰. On the other hand, seawater carbon as tracked with $\delta^{13}C_{carb}$ remains roughly constant with time, with δ^{13}Ccarb averaging about 0%.

Variation in fluxes over time within the carbon cycle can be monitored by an isotopic mass balance (Des Marais, 1997), whereby;

$$\delta_{in} = f_{carb}\delta^{13}C_{carb} + f_{org}\delta^{13}C_{org}$$

δ_{in} represents the isotopic composition of carbon entering the global surface environment comprised of the atmosphere, hydrosphere, and biosphere. The right side of the equation represents the weighted-average isotopic composition of carbonate ($\delta^{13}C_{carb}$) and organic ($\delta^{13}C_{org}$) carbon buried in sediments, and f_{carb} and f_{org} are the fractions of carbon buried in each form ($f_{carb} = 1 - f_{org}$). For timescales longer than 100 Myr, δ_{in} = -5‰, the average value for crustal and mantle carbon (Holser et al., 1988). Thus, where values of sedimentary $\delta^{13}C_{carb}$ and $\delta^{13}C_{org}$ can be measured, it may be possible to determine f_{org} for ancient carbon cycles. Higher values of $\delta^{13}C_{carb}$ indicate either a higher value of f_{org} or a greater negativity of average $\delta^{13}C_{org}$.

During the Phanerozoic, there are several peaks in δ^{13}Ccarb, the largest at about 110, 280, 300, 400, and 530 Ma (Figure 3). These peaks are widely interpreted to reflect an increase in burial rate of organic carbon (Des Marais et al., 1992; Frakes et al., 1992). This is because organic matter selectively enriched in ^{12}C depletes seawater in this isotope, raising the $\delta^{13}C$ values of seawater. In the late Paleozoic (300-250 Ma), the maxima in δ^{13}Ccarb correspond to the rise and spread of vascular land plants, which provided a new source of organic debris for burial (Condie 2106, Berner, 1987, 2001). Also conducive to preservation of

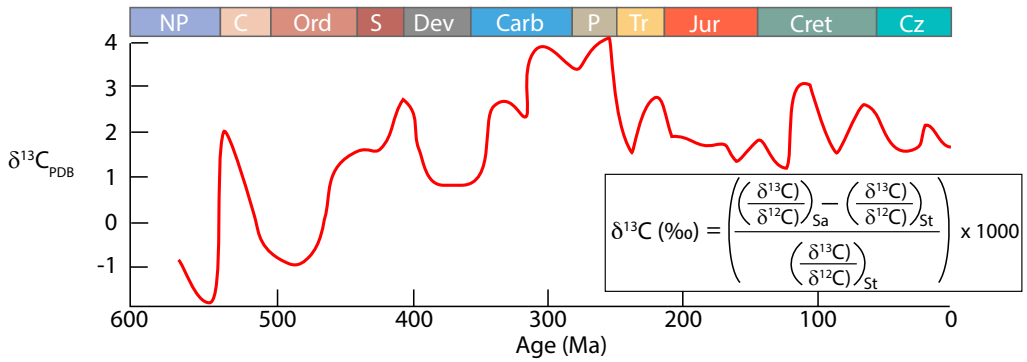

Figure 3. Secular changes in $\delta^{13}C$ in seawater in the last 600 Myr based on data from marine carbonates

organic remains at this time were the vast lowlands on Pangea, which appear to have been sites of widespread swamps where bacterial decay of organic matter is minimized. The drop in $\delta^{13}C_{carb}$ at the end of the Permian is not understood. Perhaps, large amounts of photosynthetic O_2 generated by Carboniferous forests led to extensive forest fires that destroyed large numbers of land plants in the Late Permian (Condie, 2016). However, the reasons for the oscillations in $\delta^{13}C_{carb}$ are not yet unequivocally resolved and, as in all sciences, the tenet "...perceived correlation does not necessarily equate to causation"must always be at the forefront in the scientific mindset.

Across the Precambrian and the Phanerozoic, the initiation of glaciation on a global scale, as in the Cryogenian 'Snowball Earth', has been interpreted to be dependent on parameters like the latitudinal extent of continents and oceanic circulations (Figure 4; Condie, 2016). The main drive for an onset of global glaciation is believed to be the lowering of atmospheric CO_2. It likely also requires a continental landmass to be covering one of the earth's polar positions. More recently, cooling related to an increase in the earth's albedo due to widespread evaporites (saline giants) has been added to the list of possible drivers to the onset of glaciation.

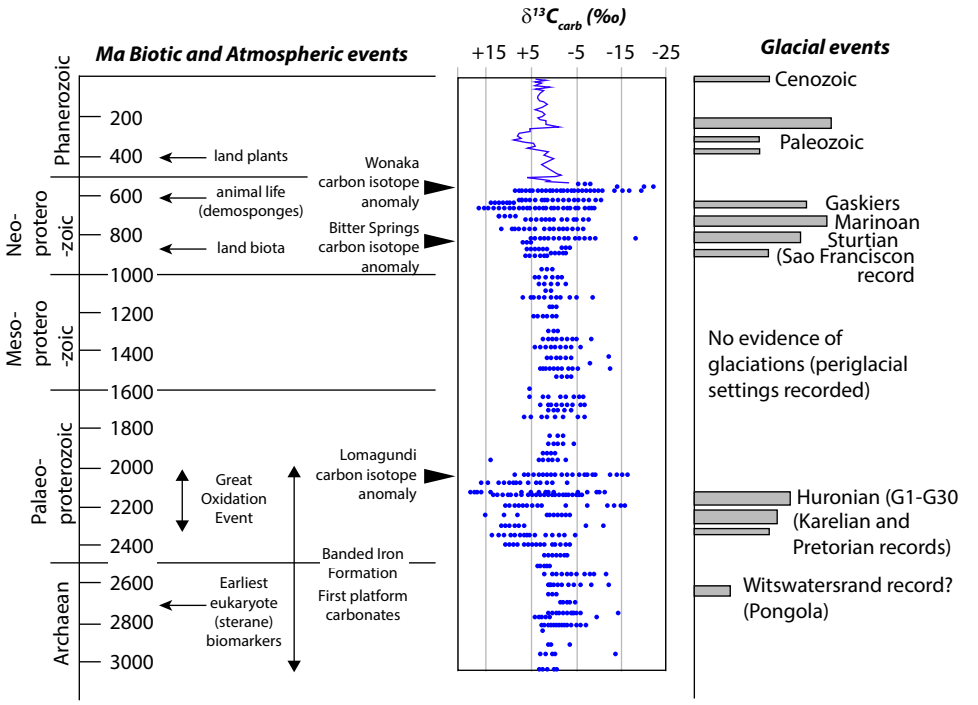

Figure 4. A summary chart of Precambrian and Phanerozoic events plotted against variation in values of $\delta^{13}C_{carb}$ (after Strand 2012), showing many but not all times of wider oscillations correspond to glacial periods in the earth's history (Strand, 2012). Proterozoic carbon isotope anomalies outside the glacial eras are the Lomagundi, Bitter Springs and Wonoka events.

Climate modelling studies imply that CO_2 concentrations as low as 100–150 ppm are required to initiate global glaciation (e.g. Liu et al., 2013; Feulner and Kienert, 2014). One potential cause of lowered CO_2 is drawdown of CO_2 during intense silicate weathering in equatorial regions (Hoffman and Schrag, 2002; Goddéris et al., 2003). Photosynthesis provides another mechanism for CO_2 drawdown, via conversion of CO_2 to O_2 and rapid burial of organic carbon, which is reflected in a positive $\delta^{13}C$ excursion for carbonates (Pierrehumbert et al., 2011). Additionally, long term cloud cover (Feulner et al., 2015), fluctuations in atmospheric-ocean heat transport, the earth's albedo, or solar luminosity (Pierrehumbert et al. (2011) are also proposed as potential causes of the onset of glaciation (ice-house mode climate).

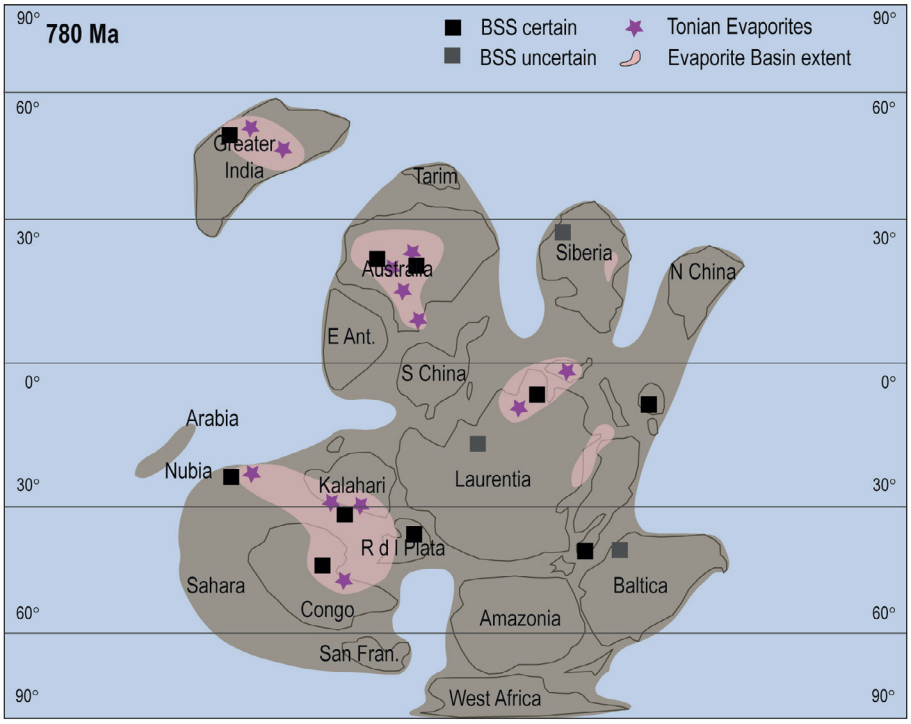

Figure 5. Extent of evaporite basins (Tonian = 780Ma) on the Rodinian supercontinent (after Li et al., 2008; Schmid, 2017).

In a recent paper, Schmid 2017 focused on the cause of the Bitter Springs carbon isotope anomaly, she argues the cause of the pre-glacial, globally recognised, carbon and oxygen isotope variations in carbonate sediments tied to the Bitter Springs anomaly is a response to widespread fractional evaporation of dissolved CO_2. This carbon isotope anomaly ties to a well defined correlation with the distribution of Neoproterozoic evaporite basins. She also shows volcanism occurred during the onset of the Bitter Springs Stage (811–788 Ma) and associated widespread evaporite distribution across Australia.

Schmid (op. cit.) argues that the albedo effect began with of the widespread deposition of Rodinian

supercontinent evaporites in very shallow marine to epicontinental sedimentary successions beginning ≈810 Ma, increased siliciclastic redbed weathering. This and continuing evaporite deposition and exposure between ≈780 and 720 Ma drove a worldscale increase in Earth's albedo. Such highly reflective salt deposits defined a saline giant across an area that today covers one-third of the Australia continent. Thus, this and other penecontemporaneous saline giants over the Rodinian supercontinent played a potentially significant role in the onset of atmospheric cooling via a significant increase in albedo (Figure 5). These salt beds occur in periods that typify the onset of local (750 Ma) and then global glaciation (720 Ma).

Schmid (2017) goes on to note that the degree of evaporation in the Bitter Springs group sediments is related to the $\delta^{13}C$ signature in variably concentrated waters (Figure 6). That is the Tonian Bitter Springs Group (≈830–750 Ma), within the Amadeus Basin in central Australia consists of thick halite and sulphate evaporite accumulations and associated carbonates. The deposition of halite occurred in shallow marine, lagoon (salina) environment (Gillen Formation), and developed into sulphate-dominated supratidal sabkha during sea level regression (Johnnys Creek Formation). The overall regression was interrupted by a transgressive phase lasting at least 20 Ma and leading to deposition of basin-wide stromatolitic dolostone (Loves Creek Formation). The salinity and high evaporation is reflected in positive $\delta^{13}C$ in the intercalated carbonates (+4 to +6‰ VPDB) of the evaporitic units, while the shallow marine stromatolitic incursion of the Loves Creek Formation (–2‰ δ13C) show typical marine carbonate isotopic values (Figure 7).

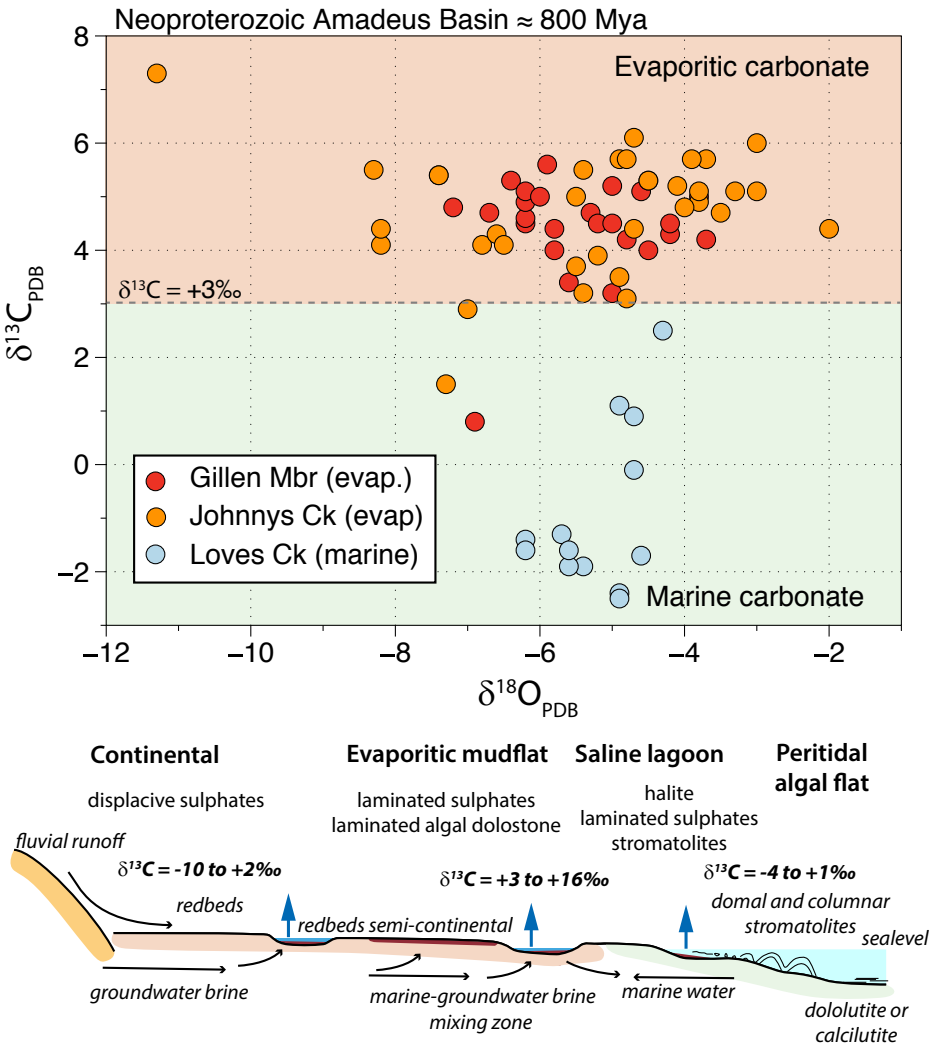

Figure 6. Carbon isotopes in evaporitic sediments of the Neoproterozoic Bitter Springs Group of the Amadeus Basin, Central Australia. A) Carbon-Oxygen crossplot showing how carbon values can separate marine versus evaporitic clusters. B) Schematic section showing separation in $\delta^{13}C$ in various carbonates in relation to their depositional environments ranging from continental redbed, supratidal salt flat (sabkha), salt lagoon (salina) and intertidal shallow marine settings (extracted from Schmid, 2017).

This salinity controlled isotopic separation supports the observations of Stiller et al. (1985) who noted extreme enrichment of ^{13}C in the dissolved inorganic carbon pool in evaporating brines up with $\delta^{13}C$ values of up to + 16.5‰ under natural abiotic, oxic conditions in Dead Sea evaporation ponds (Figure 7). The systematic increase in ^{13}C values in highly evaporated waters from the various bittern ponds of the Dead Sea Saltworks is thought to result from a nonequilibrium gas-transfer isotope fractionation. The process of ongoing evaporation leads to CO_2 loss within the evaporative brine as less and less gas can held in solution (see Warren 2016, Chapter 9). CO_2 exchange in a concentrating surface brine occurs directly between the water column and air, resulting in direct CO_2 loss through evaporation. In a sabkha environment. CO_2 is released from the hypersaline groundwater through sediments before being released to air as evaporites may form intrasediment precipitates. Overall, atmospheric CO_2 uptake in hypersaline settings fed by shallow marine water is diminished compared to the normal marine settings.

Precipitated carbonates modern salinas and sabkhas are mainly aragonite, and formed in association with such evaporative brine, are consistently ^{13}C enriched, as seen in nearby Solar Lake and Sabkha Gavish (Figure 2; Stiller et al., 1985; Schidlowski et al., 1984). In a similar fashion, Palaeoproterozoic interbedded shallow marine carbonates, redbeds and evaporites have values up to $\delta^{13}C$ + 17.2‰ (Melezhik et al., 1999). Permian and Triassic (Schmid et al., 2006a) redbeds and evaporite sequences also have ^{13}C-rich carbonates (up to +7‰) and enrichment is partly attributed to evaporation and associated CO_2 loss (Beauchamp et al., 1987). In modern oceans, atmospheric CO_2 is consumed by biological activity and carbonate production originates from mainly marine organisms, leading to near atmospheric to organic negative $\delta^{13}C$ signatures in the precipitated sediment(Andersson, 2013).

If increasing salinity leads to unfavourable conditions for photosynthesising organisms to survive (Lazar and Erez, 1992), carbonate through to bittern precipitation becomes increasingly abiotic and evaporation driven,

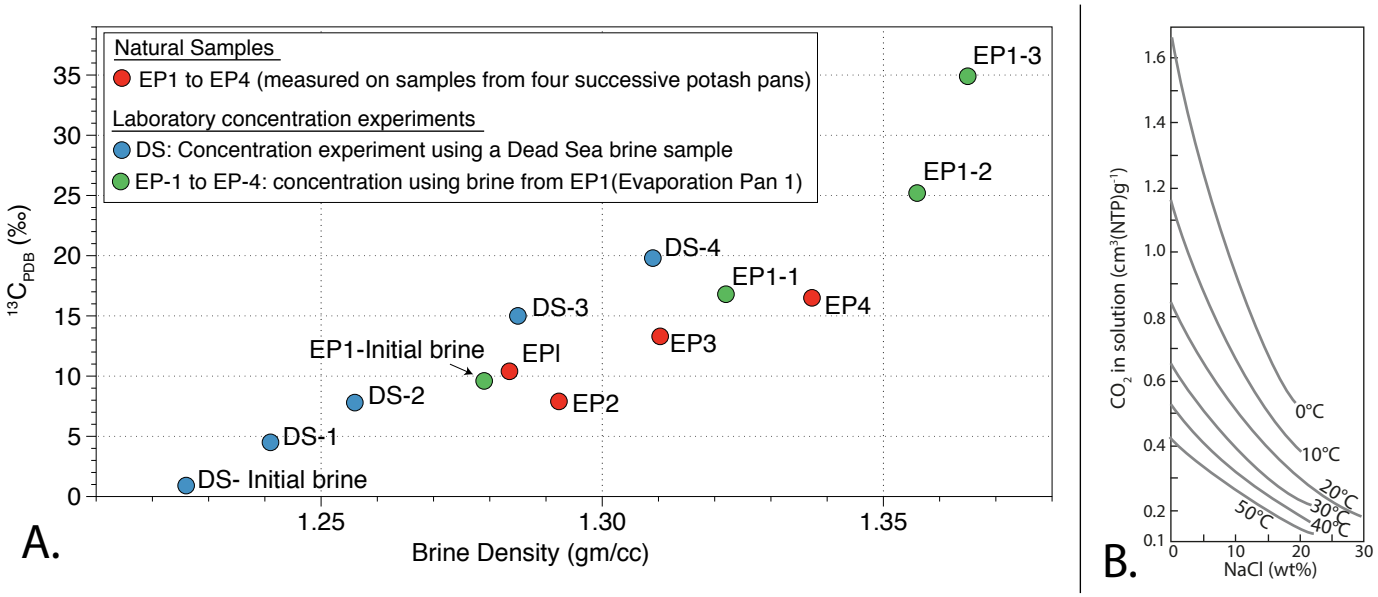

Figure 7. A. ^{13}C measured in dissolved inorganic carbon collected from a series of bittern pools in the Dead Sea Salt Works and laboratory determinations (after Stiller et al., 1985). B) CO_2 solubility variations with respect to temperature and NaCl concnetration (after Schidlowski et al., 1984).

especially at the upper end of the evaporation series. The loss of Ca during evaporation of a brine, via aragonite and calcium sulphate precipitation, leads to an increase in Mg/Ca ratio and an increase in residual brine density. This can result in primary dolomite precipitation or widespread reflux dolomitisation (Schmid et al., 2006, Warren 2000, 2016).

In summary, the typical $\delta^{13}C$ signature in normal marine carbonate sediment across much of geological time centres around 0 ‰ and ranges between a few parts per mille on either side of the zero line reflecting precipitation by calcifying and photosynthesising organisms (e.g. algae), while abiotic, evaporation induced carbonates tend to have $\delta^{13}C$ values above +1‰. More positive $\delta^{13}C$ values (+4 to +6‰) tend to typify dominantly abiotic carbonates (and local methanogenic carbonates with even more positive values) and support the notion of evaporation-driven 13C-enrichement in times of widespread evaporitic epeiric and basinwide carbonates. In the Precambrian, widespread marine stromatolitic units such as, algal Loves Creek Formation reflects $\delta^{13}C$ values for biogenic carbonate precipitation under shallow marine, non-hypersaline conditions. The change from a shallow hypersaline lagoon towards evaporitic mudflats and salterns suggests an increase in aridity and continentality/hydrographic isolation, with associated more positive $\delta^{13}C$ values.

Implications for some types of ^{13}C anomaly

The Bitter Springs Group chemostratigraphy has been correlated globally and the negative excursion was named previously after this unit (Bitter Springs Stage anomaly). However, the mechanism of evaporation-driven fractionation of δ13C is different from the commonly proposed inorganic-organic carbon fractionation, and challenges the views on interpreting global chemostratigraphic anomalies or excursion and their cause. Evaporite basins covered vast regions worldwide prior to the Sturtian glaciation, e.g. the Australian evaporites would have covered a third of the continent. The light surface of evaporites and associated carbonates would have had a high albedo and effectively cause less surface heat absorption. This subsequently would have triggered temperature decrease on a continental and possibly global scale. The Schmid paper hypothesises that the deposition of evaporites worldwide would have contributed to global cooling starting ≈100 Ma prior to Snowball Earth and would have played an important role in the onset of global glaciation.

References

Andersson, A.J., 2013. The oceanic CaCO3 cycle. In: T. Holland (Editor), Treatise on Geochemistry, 2nd ed. Elsevier, pp. 519-542.

Beauchamp, B., Oldershaw, A.E. and Krouse, H.R., 1987. Upper Carboniferous to Upper Permian 13C-enriched primary carbonates in the Sverdrup Basin, Canadian Arctic: comparisons to coeval western North American ocean margins. Chem. Geol. , 65: 391-413.

Berner, R.A., 1987. Models for carbon and sulfur cycles and atmospheric oxygen; application to Paleozoic geologic history. American Journal of Science, 287: 177-196.

Berner, R.A., 2001. Modeling atmospheric O2 over Phanerozoic time. Geochimica et Cosmochimica Acta, 65: 685-694.

Condie, K.C., 2016. Earth as an Evolving Planetary System (3rd edition). Elsevier, 350 pp.

Des Marais, D.J., 1997. Isotopic evolution of the biogeochemical carbon cycle during the Proterozoic Eon. Organic Geochemistry, 27(5): 185-193.

Des Marais, D.J., Strauss, H., Summons, R.E. and Hayes, J.M., 1992. Carbon isotope evidence for the stepwise oxidation of the Proterozoic environment. Nature, 359: 605-609.

Feulner, G., Hallmann, C. and Kienert, H., 2015. Snowball cooling after algal rise. Nat. Geosci. , 8: 659-662.

Feulner, G. and Kienert, H., 2014. Climate simulations of Neoproterozoic snowball Earth events: similar critical carbon dioxide levels for the Sturtian and Marinoan glaciations. Earth Planet. Sci. Lett., 404: 200-205.

Frakes, L.A., Francis, J.E. and Syktus, J.L., 1992. Climate modes of the Phanerozoic. Cambridge University Press, New York, 274 pp.

Goddéris, Y., Donnadieu, Y., Nédélec, A., Dupré, B., Dessert, C., Grard, A., Ramstein, G. and François, L.M., 2003. The Sturtian 'snowball' glaciation: fire and ice. Earth Planet. Sci. Lett. , 211: 1-12.

Hoffman, P.F. and Schrag, D.P., 2002. The snowball Earth hypothesis: testing the limits of global change. Terra Nova, 14: 129-155.

Holser, W.T., Schidlowski, M., Mackenzie, F.T. and Maynard, J.B., 1988. Geochemical cycles of carbon and sulfur. In: C.B. Gregor, R.M. Garrels, F.T. Mackenzie and J.B. Maynard (Editors), Chemical cycles in the evolution of the earth. John Wiley, New York, pp. 105–173.

Horton, T.W., Defliese, W.F., Tripati, A.K. and Oze, C., 2016. Evaporation induced 18O and 13C enrichment in lake systems: A global perspective on hydrologic balance effects. Quaternary Science Reviews, 131: 365-379.

Lazar, B. and Erez, J., 1992. Carbon geochemistry of marine-derived brines: I. 13C depletions due to intense photosynthesis. Geochim. Cosmochim. Acta, 56: 335-345.

Leng, M.J. and Marshall, J.D., 2004. Paleoclimate interpretation of stable isotope data from lake sediment archives. Quaternary Science Reviews, 23(811-831).

Liu, Y., Peltier, W.R., Yang, J. and Vettoretti, G., 2013. The initiation of Neoproterozoic ''snowball'' climates in CCSM3: the influence of paleocontinental configuration. Climate Past, 9: 2555-2577.

Melezhik, V.A., Fallick, A.E., Medvedev, P.V. and Makarikhin, V.V., 1999. Extreme 13Ccarb enrichment in ca. 2.0 Ga magnesite-stromatolite-dolomite-'red beds' association in a global context: a case for the world-wide signal enhanced by a local environment. Earth Sci. Rev., 48: 71-120.

Pierrehumbert, R.T., Abott, D.S., Voigt, A. and Koll, D., 2011. Climate of the neoproterozoic. Annu. Rev. Earth Planet. Sci., 39: 417-460.

Schidlowski, M., Matzigkeit, U. and Krumbein, W.E., 1984. Superheavy organic carbon from hypersaline microbial mats; Assimilatory Pathway and Geochemical Implications. Naturwissenschaften, 71(6): 303-308.

Schmid, S., 2017. Neoproterozoic evaporites and their role in carbon isotope chemostratigraphy (Amadeus Basin, Australia). Precambrian Research, 290: 16-31.

Schmid, S., Worden, R.H. and Fisher, Q., 2006. Carbon isotope stratigraphy using carbonate cements in the Triassic Sherwood Sandstone Group: Corrib Field, west of Ireland. Chem. Geol., 225: 137-155.

Stiller, M., Rounick, J.S. and Shasha, S., 1985. Extreme carbon-isotope enrichments in evaporating brines. Nature, 316: 434.

Swart, P.K., 2015. The geochemistry of carbonate diagenesis: The past, present and future. Sedimentology, 62(5): 1233-1304.

Warren, J.K., 2000. Dolomite: Occurrence, evolution and economically important associations. Earth Science Reviews, 52(1-3): 1-81.

Warren, J.K., 2016. Evaporites: A compendium (ISBN 978-3-319-13511-3). Springer, Berlin, 1854 pp.

Worsley, T.R. and Nance, R.D., 1989. Carbon redox and climate control through Earth history: A speculative reconstruction. Paleogeography, Paleoclimatology, Paleoecology, 75: 259-282.

Saltworks Consultants Pty Ltd
ABN 068 889 127
Kingston Park,
5049 South Australia

Email: enquiries@saltworkconsultants.com

Web Page: www.saltworkconsultants.com